RESEARCH ARTICLE

Macromolecular Rapid Communications

www.mrc-journal.de

Anomalous Loss of Stiffness with Increasing Reinforcement in a Photo-Activated Nanocomposite

*Hongyuan Zhu, Tian Jian Lu, Feng Xu, Guy M. Genin, and Min Lin**

Hydrogels are commonly doped with stiff nanoscale fillers to endow them with the strength and stiffness needed for engineering applications. Although structure–property relations for many polymer matrix nanocomposites are well established, modeling the new generation of hydrogel nanocomposites requires the study of processing–structure–property relationships because subtle differences in chemical kinetics during their synthesis can cause nearly identical hydrogels to have dramatically different mechanical properties. The authors therefore assembled a framework to relate synthesis conditions (including hydrogel and nanofiller mechanical properties and light absorbance) to gelation kinetics and mechanical properties. They validated the model against experiments on a graphene oxide (GO) doped oligo (ethylene glycol) diacrylate (OEGDA), a system in which, in apparent violation of laws from continuum mechanics, doping can reduce rather than increase the stiffness of the resulting hydrogel nanocomposites. Both model and experiment showed a key role light absorbance-dominated gelation kinetics in determining nanocomposite mechanical properties in conjunction with nanofiller reinforcement, with the nanofiller's attenuation of chemical kinetics sometimes outweighing stiffening effects to explain the observed, anomalous loss of stiffness. By bridging the chemical kinetics and mechanics of nanocomposite hydrogels, the authors' modeling framework shows promise for broad applicability to design of hydrogel nanocomposites.

1. Introduction

Hydrogels, water-immersed hydrophilic polymer networks, are important across a broad range of technologies including tissue engineering, drug delivery, and soft electronics.[1] The ability of hydrogels to provide components of defined shape and stiffness has been central to the emergence of the fields of mechanobiology[2] and soft robotics.[3] However, application of hydrogels is often limited by their relatively low toughness and stiffness.[4] Much effort has thus been devoted to engineering stiffer and tougher hydrogels by increasing crosslink density,[5] employing double networks,[6] dual cross-linking,[7] or doping to create nanocomposite hydrogels.[8] Nanocomposite hydrogels are particularly attractive because nanofillers, reinforcing particles with at least 1D below 100 nm, can endow hydrogels additional functionalities such as improved optical absorbance, thermal stability, electrical conductivity, and magnetic properties.[9]

Nanofillers of many concentrations, shapes, and mechanical properties have been incorporated into hydrogels, including 0D nanoparticles (e.g., noble metals[10] and silica[11]); 1D nanofibers (e.g., carbon nanotubes[12] and cellulose fibers[13]); and 2D nanosheets (e.g., graphene oxides[14] and clay sheets[15]). Nanofillers affect the final mechanical properties of nanocomposite hydrogels in two ways: i) by altering the gelation kinetics and thus the final crosslinking density of the hydrogels; and ii) by altering the local stress and strain field of the hydrogels. Optimization of nanocomposite hydrogels typically

Dr. H. Zhu, Prof. F. Xu, Prof. G. M. Genin, Prof. M. Lin
The Key Laboratory of Biomedical Information Engineering of Ministry of Education
School of Life Science and Technology
Xi'an Jiaotong University
Xi'an 710049, P. R. China
E-mail: minlin@mail.xjtu.edu.cn

Dr. H. Zhu, Prof. F. Xu, Prof. G. M. Genin, Prof. M. Lin
Bioinspired Engineering & Biomechanics Center (BEBC)
Xi'an Jiaotong University
Xi'an 710049, P. R. China

Prof. T. J. Lu
State Key Laboratory of Mechanics and Control of Mechanical Structures
Nanjing University of Aeronautics and Astronautics
Nanjing 210016, P. R. China

Prof. T. J. Lu
MOE Key Laboratory for Multifunctional Materials and Structures
Xi'an Jiaotong University
Xi'an 710049, P. R. China

Prof. G. M. Genin
Department of Mechanical Engineering & Materials Science
Washington University in St. Louis
St. Louis, MO 63130, USA

Prof. G. M. Genin
NSF Science and Technology Center for Engineering Mechanobiology
Washington University in St. Louis
St. Louis, MO 63130, USA

The ORCID identification number(s) for the author(s) of this article can be found under https://doi.org/10.1002/marc.202100147

DOI: 10.1002/marc.202100147

proceeds to at least some degree by trial and error, and sometimes out of the scope of the common senses of mechanics (e.g., modulus could reduce by increasing the doping content),[16–18] in part because a comprehensive model for predicting gelation kinetics and mechanical properties does not yet exist. Although structure–function relationships that relate material composition and architecture to mechanical properties are well established, these are often inadequate for hydrogel nanocomposites, because nearly identical hydrogels can have dramatically different properties based upon subtle differences in the kinetics of their synthesis.[19] We demonstrate here this by presenting an integrated synthesis–structure–function model that accounts for how gelation kinetics affects final mechanical properties in a hydrogel nanocomposite system, and applying it to explain a novel phenomenon observed in our experiments, in which increasing the concentration of a fully bonded, well distributed stiff reinforcing phase can, under certain conditions of light illumination during synthesis, reduce the stiffness of the final hydrogel nanocomposite.

Gelation of hydrogels due to free radical polymerization arises through three main chemical reactions: i) radical generation from the decomposition of initiators (including photoinitiators and thermal initiators etc.); ii) radical propagation to monomers with extension of the polymer chain; and iii) radical termination as two radical species reacted.[20] The associated kinetics can be predicted by a set of ordinary differential equations (ODEs) describing detailed chemical reactions with kinetic constants that depend on both the composition of precursors and the experimental conditions of the reaction, including temperature, pH, and light intensity.[19,21,22] These kinetic processes determine the nanoscale network topology (e.g., crosslinks, loops, dangle chains) and then the mechanical properties of the hydrogels.[19,21,22] These well-known processes all change for the case of nanocomposite hydrogels. Nanofillers are believed to affect gelation kinetics by acting as proton donors for radical generation,[23,24] as radical scavengers,[25,26] or as diffusion barriers.[27,28] A range of ordinary differential equation (ODE) based radical gelation kinetics models for nanocomposite hydrogels have been developed that track the time evolution of monomer conversion as an indicator of gelation kinetics, and that adjust one or several adjustable kinetic constants to fit the experimental observations.[25,29] However, no comprehensive model yet exists that considers how nanofillers affect light absorption and predicts the final mechanical properties of the nanocomposite hydrogel.

Continuum homogenization models methods for predicting the enhancement of mechanical properties by inclusions with defined mechanical properties, geometries, and distributions are well-established. These general theories estimate how macroscopic material properties are affected by microscopic localizations of stress around filler particles[30] by assuming that: i) fillers and matrix are linear elastic; ii) filler particles are identical in shape; iii) fillers and matrix are perfectly bonded; and iv) the filler does not alter the mechanical properties of the matrix.[30–32] Note that this latter factor is frequently violated by nanoscale particles with high surface energy.[19] Homogenization methods fall into two categories: bounds and estimates.[30,32–34] Bounds such as the Voigt and Reuss bounds,[35,36] Hashin–Shtrikman bounds,[37,38] and three-point bounds[30,39] establish upper and lower limits on stiffening of elastic materials by filler; estimates such as the self-consistent method,[40,41] the Halpin–Tsai equations[42,43] and the Mori–Tanaka model,[44–48] provide estimates within these bounds, typically based on a combination of the Eshelby solution for an isolated ellipsoidal inclusion embedded in an infinite medium[49] with various of effective-medium approximations that model interactions between inclusions. Most particulate-reinforced materials parallel the Hashin–Shtrikman lower bound at low volume fraction of filler and the Mori–Tanaka estimate that we use in this work does as well.

Although classical continuum homogenization theories predict no effect of reinforcement size on composite stiffness,[50] certain nanocomposites, such as graphene-doped polymer matrix nanocomposites, exhibit higher stiffness with smaller reinforcing particles, including stiffness exceeding classical upper bounds for composite moduli.[18,19,51,52] The reason for this is that effects of surface energy become important as surface area increases with smaller reinforcing particles for reinforcement of a prescribed volume fraction. This effect that has been modeled for linear nanocomposite materials using extensions of the Gurtin–Murdoch model.[53–56] Therefore, to model how surface energy at the filler-matrix interface affects the effective moduli of hydrogel nanocomposites, we adopted an elastic theory based upon the Gurtin–Murdoch model.

Our comprehensive model combined theories of gelation kinetics and micromechanics to predict how the mechanical properties of a nanocomposite hydrogel arise from the precursor solution, the shape and mechanics of nanofillers, and the intensity and duration of irradiation during photo-crosslinking (**Figure 1**, see Supporting Information for both modeling and experimental details). The photocrosslinkable nanocomposite hydrogel precursor chosen as a model system was a mixture of eosin Y (EY), triethanolamine (TEOA), oligo (ethylene glycol) diacrylate (OEGDA), and graphene oxide (GO). The model was verified by Fourier transform infrared (FTIR) spectrometry to quantify gelation kinetics and nanoindentation to quantify effective elastic moduli of nanocomposite hydrogels. Then the validated model was applied to explore parameter space and demonstrate how nanofiller concentration, shape, modulus, and surface affect the mechanical properties of the nanocomposite hydrogel, thereby demonstrating how our model can provide a general guidance for engineering nanocomposite hydrogels.

2. Results and Discussion

To quantify the mechanisms underlying the well-known effects of GO dopant on the absorption coefficient and gelation process,[18,25] we used FTIR to determine the irradiation time-dependent fractional concentration of acrylate ($X_{CC}(t)$) as a function of GO concentration ([GO]) with a sample thickness (Z_{max}) fixed at 0.17 mm. GO accelerated gelation kinetics at lower concentrations of [GO] (0–5.8 mg ml^{-1}) with the rate of consumption of acrylate increased, but retarded gelation kinetics at higher concentrations of [GO] (**Figure 2**a).

We hypothesized that this non-monotonic effect of GO arose from the optical absorption and surface chemistry of GO. To separate these factors, we increased sample thickness (Z_{max} = 1.02 mm) while keeping all other factors the same so that surface chemistry would remain identical while optical absorption by GO

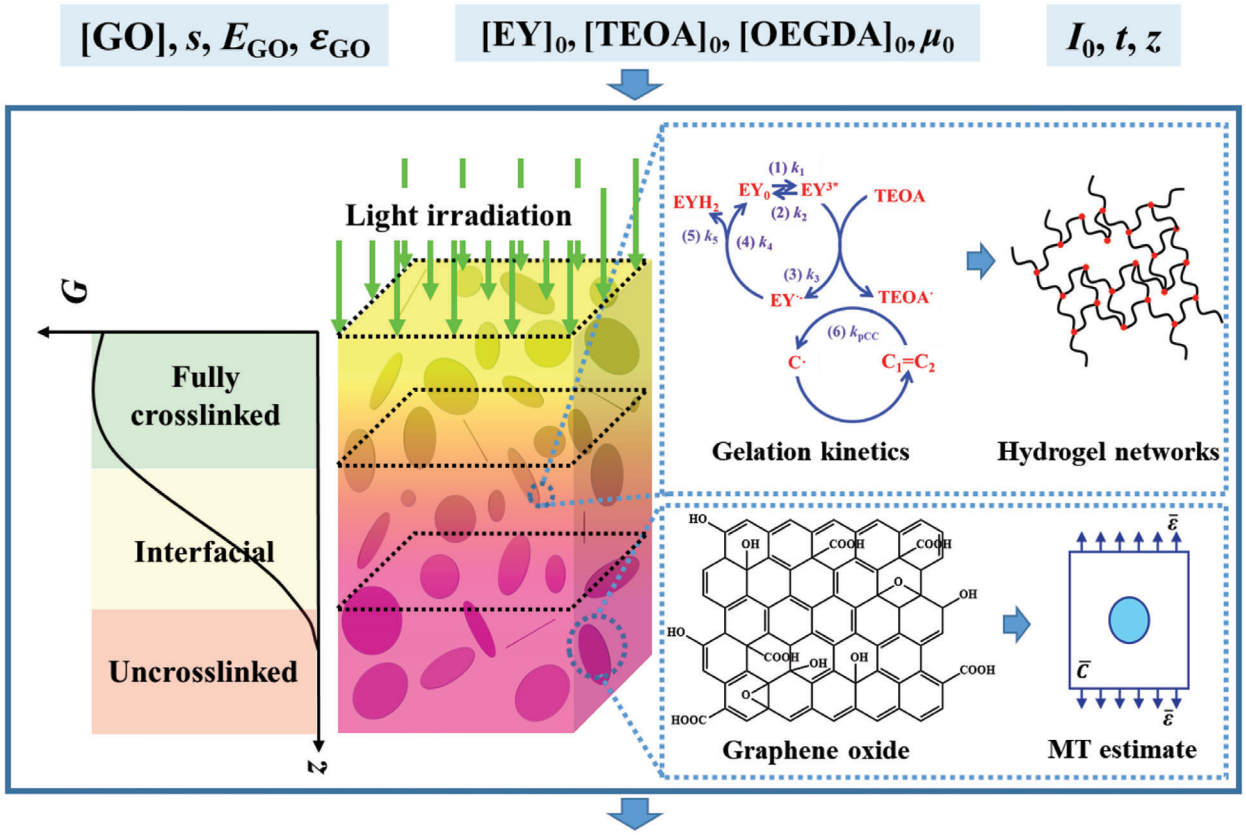

Figure 1. Schematic of a model for how gelation kinetics and micromechanics combine to determine the mechanical properties of GO-OEGDA. Mechanical properties are determined by the effects of nanofiller on both gelation kinetics and micromechanics, depending on light absorbance, aspect ratio and modulus of nanofiller, composition, and light absorbance of the hydrogel matrix and gelation conditions. When GO-OEGDA samples of a prescribed thickness are irradiated by light, a gradient in the elastic modulus will form in the irradiation direction due to light intensity attenuation. Photobleaching could leada reverse stiffness gradient at the surface.[22] The elastic modulus of the hydrogel matrix (E_m) is determined by gelation kinetics, which is a function of both initiator and GO concentrations. The elastic modulus of GO-OEGDA nanocomposites (E_c) can, in certain conditions, be calculated by continuum estimates such as the Mori–Tanaka (MT) estimate based upon the size, shape, and modulus of the nanofiller, and upon E_m.

would be amplified (Figure 2b). The acrylate consumption rate was insensitive to sample thickness in the absence of GO, but was retarded in the thicker sample for [GO] = 11.6 mg ml^{-1}. These effects were captured by our gelation kinetics model (Equation S10, Supporting Information). R_{i0} varied with [GO] following a biphasic relationship (dots in Figure 2c), as expected because GO serves both as a hydrogen donor for radical generation[23,24] and as a scavenger of primary radicals.[25,26] It also varies with light intensity, which decreases with sample depth due to light absorption. In order to capture the experimentally observed R_{i0} as varying [GO] and Z, a fitting equation is proposed:

$$R_{i0} = \alpha \exp\left(\beta_1[\mathrm{GO}]^2 + \beta_2[\mathrm{GO}] + \beta_3\right) \exp\left(-\mu Z\right) \quad (1)$$

where α and $\beta_1 - \beta_3$ are phenomenological fitting parameters, and μ is the [GO]-dependent absorption coefficient of the nanocomposite hydrogel. $\beta_1 - \beta_3$ were fit from data in Figure 2a,b for both sample thicknesses (dots in Figure 2c), μ was and fit to UV–vis spectrum measurements for hydrogel precursors with different [GO] (hollow dots, Figure 2d) following the Beer–Lambert law:

$$\mu = \epsilon_{GO}\ [\mathrm{GO}] + \mu_0 \quad (2)$$

where ϵ_{GO} is the absorbance per unit [GO] and μ_0 is the absorption coefficient of the OEGDA hydrogel precursor without GO. The fits for these models validated the kinetic framework and enabled estimate of R_{i0} at the sample surface (dashed line in Figure 2c). As predicted, R_{i0} increased with [GO] up to [GO] = 5.8 mg ml^{-1} for an over sevenfold increase in gelation rate relative to undoped OEGDA ([GO] = 0), and reduced from this peak thereafter. As a result, both sample thickness (Z) and concentration of graphene oxide ([GO]) can be used to tune gelation kinetics by altering the chemical and optical properties of GO.

Although the stiffness of a nanocomposite hydrogel is widely understood to increase monotonically with increasing concentration of stiff nanofillers,[43,48] we and others have observed anomalies in which the stiffness of the hydrogel can be reduced by a stiff nanofiller.[17,18] In our GO-OEGDA system, the Young's modulus (E_c) on the surface, measured by AFM, increased with irradiation time and increased with [GO] for lower [GO], but decreased with increasing [GO] for higher [GO] (symbols in **Figure 3**a). The model captured the experimental data (curves in Figure 3a), suggesting that the physics of underlying this related to the trade-off we modeled between chemical and optical properties of GO within OEGDA.

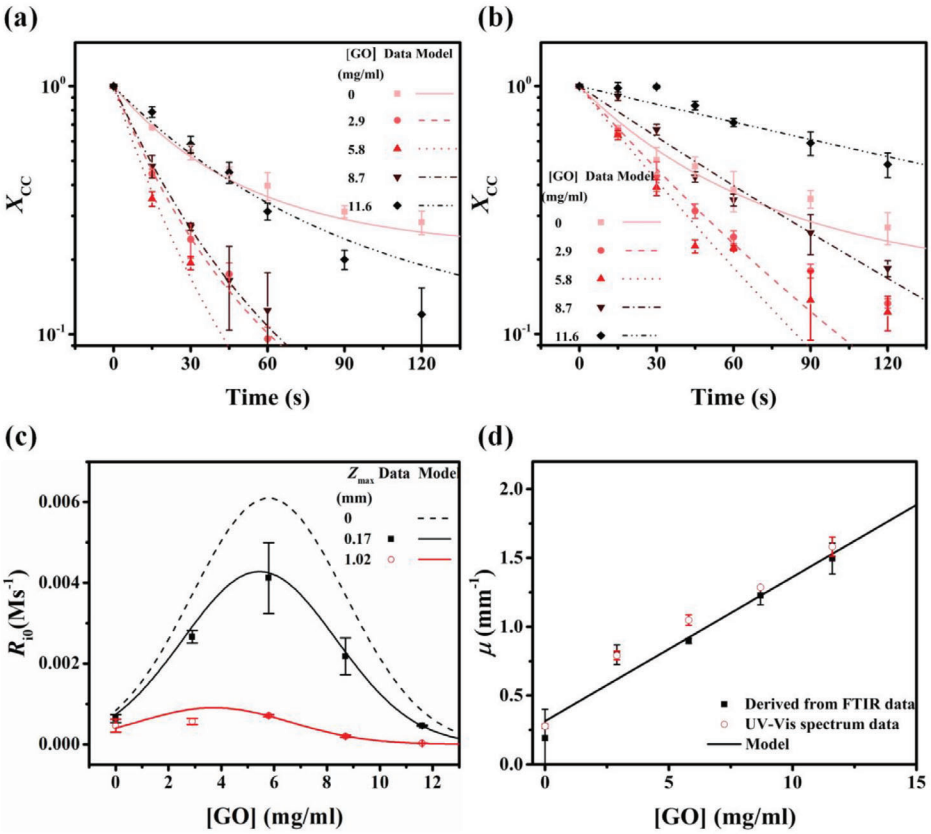

Figure 2. The effect of GO on gelation kinetics and optical absorption. a,b) The time evolution of the fractional concentration of acrylates (X_{CC}) in a hydrogel doped with different GO concentrations ([GO]) with a sample thickness (Z_{max}) of a) 0.17 mm, and b) 1.02 mm. Data represented by markers were determined by FTIR measurements; curves represent results of our fitted model. c) The dependence of initial initiation rate (R_{i0}) on [GO] for specimens of different thicknesses Z_{max}. Markers represent experimental results calculated from the slope of the curves shown in panels (a) and (b), and curves represent predictions of our fitted model. d) The dependence of the absorption coefficient (μ) on [GO]. The solid markers represent FTIR data from panels (a) and (b); the hollow markers represent data measured at 520 nm from a UV–vis spectrum; the curve represents predictions of from our fitted model.

To further understand this bi-phasic relationship, we studied the effects of optical attenuation and mechanical reinforcement independently. Acrylate conversion (P_{CC}) varied with [GO] and irradiation time similarly to R_{i0} (Figure 3b), with a peak at [GO] = 5.8 mg ml^{-1}. The time evolution curves of E_c as a function of [GO] (Figure 3c) followed the trends observed for X_{CC} (Figure 3a), further highlighting the role of gelation kinetics in composite mechanical properties.

To distinguish the effects of micromechanics, we plotted E_c – P_{CC} curves for nanocomposite hydrogels with different [GO] (Figure 3d). P_{CC} increased monotonically with E_c for all values of [GO], especially beyond a percolation threshold of P_{CC} = 0.4. For P_{CC} = 100%, the Young's modulus of GO-OEGDA doped with 11.6 mg mL^{-1} GO was predicted to be over twice that of undoped OEGDA. These monotonic trends indicate that optical effects that attenuate acrylate conversion are the source of the anomalous reduced stiffening with increased GO.

The biphasic kinetics suggest an optimum irradiation time for each value of [GO] and sample thickness for the purpose of maximizing stiffness (**Figure 4**). For a fixed thickness of Z_{max} = 0.17 mm, the final conversion of pristine OEGDA plateaued at about 80%, as determined by light intensity and initiator concentrations. This could be enhanced or attenuated by GO. At 1000 s of irradiation time, [GO] = 9.3 mg ml^{-1} was the optimum, with P_{CC} = 98% and E_c reaching 540 kPa, almost 4 times larger than that of undoped OEGDA (140 kPa, P_{CC} = 81%). For higher concentrations, optical effects could yield a composite that was less stiff than OEGDA without filler (Figure 4a).

The optical effects that underlie this anomalous material behavior are further evident from studying Young's modulus as a function of with depth Z_{max} and [GO] at a fixed irradiation time of 1000 s (Figure 4b). For the range of [GO] studied the predicted maximum E_c was not at the surface of the sample due to photobleaching of the photoinitiator. In undoped OEGDA hydrogels, the thickness of the "fully cured region" in which Young's modulus exceeded that on the surface could reach 8.3 mm. As [GO] increasing, thickness effects increased due to the Beer–Lambert phenomenon, and the thickness of the "fully cured region" decreased with [GO]. These results show a dominant role of optical effects in determining the effects of GO reinforcement on hydrogel stiffening.

We next asked what role the stiffness and shape of the nanofiller has on hydrogel mechanics by exploring the Mori–Tanaka approach used to estimate E_c. Although both factors are well known to affect the composite properties in general,[43,48,57] the strong contrast between the moduli of the filler and hydrogel

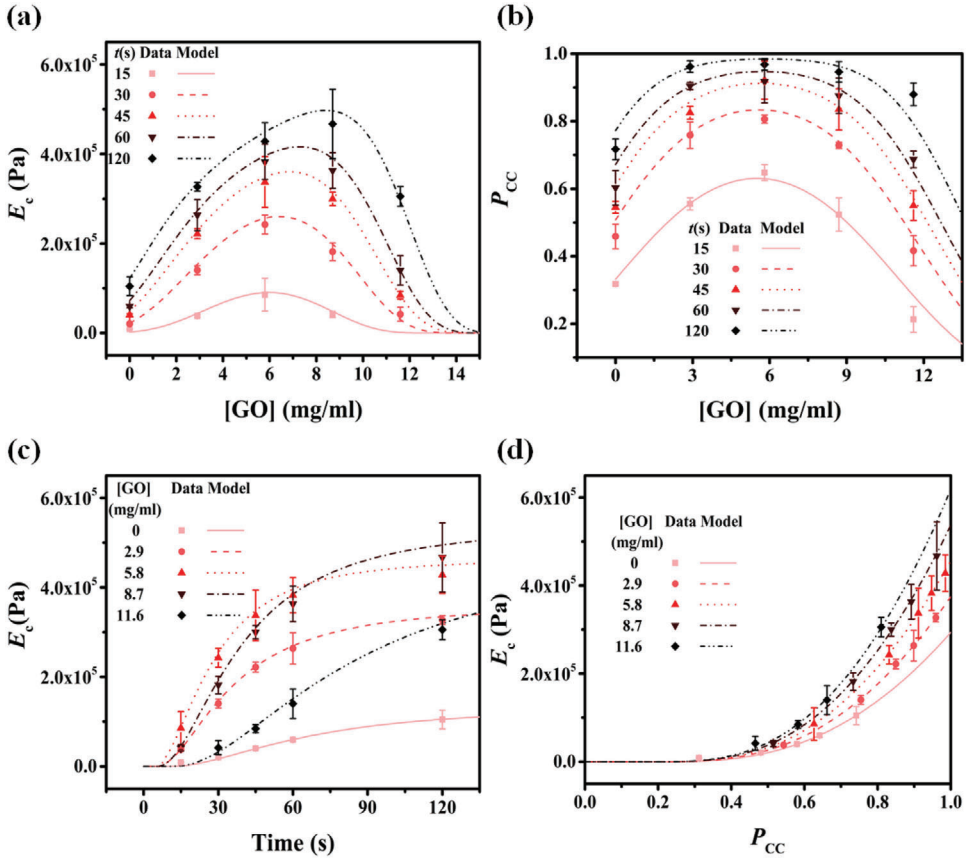

Figure 3. Gelation kinetics determine the elasticity of GO-OEGDA. A comparison of experimental data (markers) and our fitted model (curves). a) The dependence of Young's modulus of GO-OEGDA (E_c) on GO concentration ([GO]) at different irradiation times (t). b) The dependence of acrylate conversion (P_{CC}) on [GO] at different irradiation times. c) The time evolution of E_c in GO-OEGDA nanocomposites doped with different [GO]. d) E_c as a function of P_{CC} in GO-OEGDA nanocomposites doped with different [GO]. All experiments and modeling results were obtained from samples with thickness $Z_{max} = 0.17$ mm.

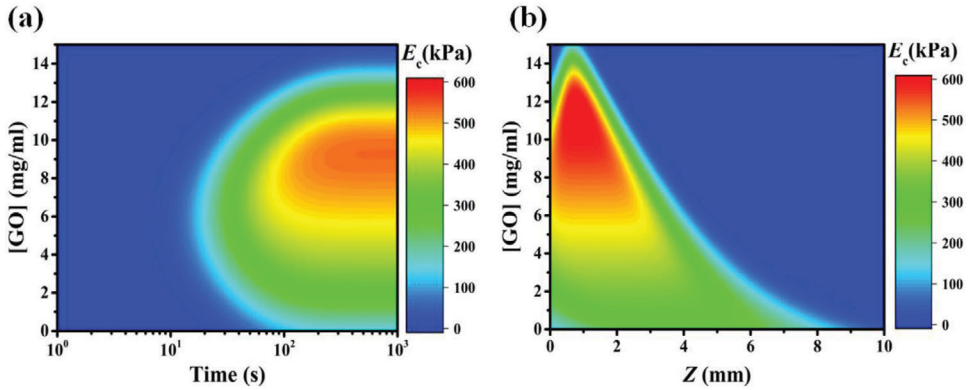

Figure 4. The Young's modulus of GO-OEGDA hydrogel nanocomposites vary with GO concentration ([GO]), irradiation time (t) and sample thickness (Z_{max}). a) Contours of E_c as a function of [GO] and irradiation time t for samples of thickness $Z_{max} = 0.17$ mm. b) Contours of E_c as a function of [GO] and depth Z for a GO-OEGDA hydrogel nanocomposite irradiated for $t = 1000$ s.

matrix makes little difference on E_c (≈6–9 orders of magnitude, blue region in **Figure 5**a). For [GO] = 11.6 mg ml^{-1} and aspect ratio $s = 0.002$, as is appropriate for the GO nanofiller used, the peak stiffening by the nanofiller was just over twice the stiffness of OEGDA, as observed in Figure 3d. This explains previous observations in the literature of composite modulus that was largely independent of filler-matrix modulus ratio E_f/E_m.[57,58] Within the range achievable by GO, stiffening can be enhanced by reducing the aspect ratio (Figure 5b). GO can be synthesized as a single atomic layer (≈0.35 nm) in sheets with dimensions of

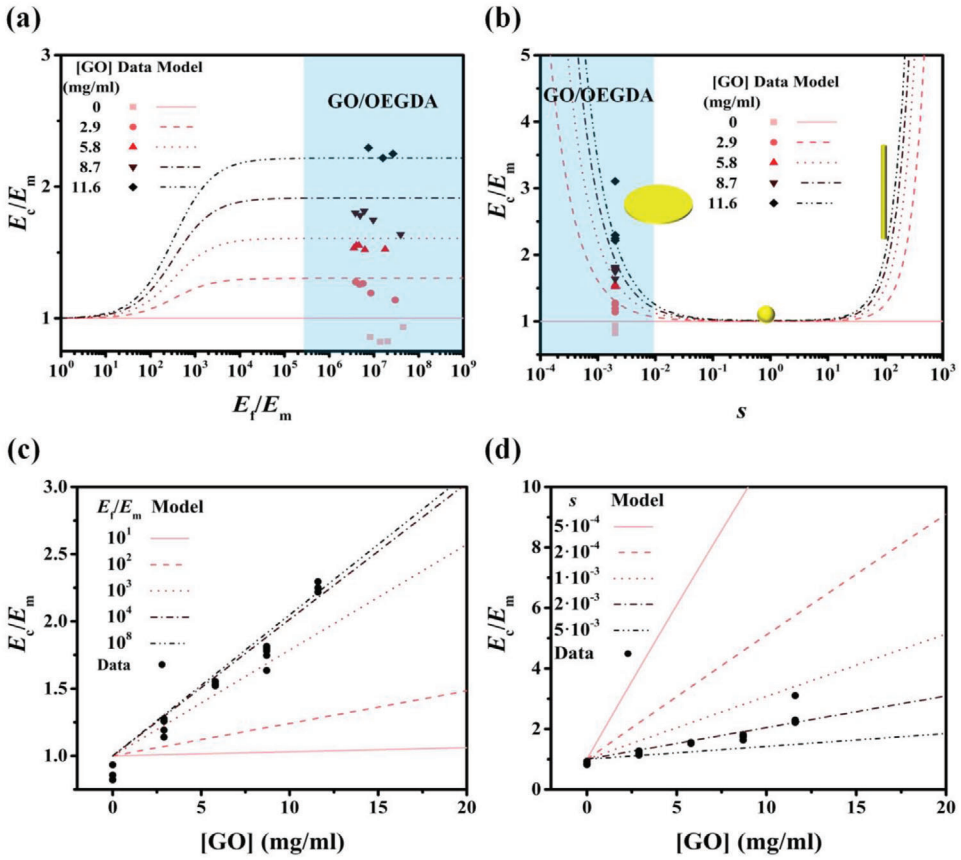

Figure 5. The dependence of Young's modulus of GO-OEGDA nanocomposite hydrogels on the shape and stiffness of GO according to the Mori–Tanaka estimate. a) The dependence of E_c/E_m on E_f/E_m for PCHs doping with varying [GO] and fixed GO aspect ratio (s) of 0.002. b) The dependence of E_c/E_m on s for GO-OEGDA nanocomposite hydrogels doped with varying [GO] with E_f/E_m fixed at 10^8. The Blue regions in (a) and (b) represent the variation range of E_f/E_m and s, respectively. c) The dependence of E_c/E_m on [GO] with varying E_f/E_m. d) The dependence of E_c/E_m on [GO] with varying aspect ratios of GO. In all the data, E_m are calculated from mean values of P_{CC} from the FTIR experiments, E_c are mean values from nanoindentation experiments, and E_f is fixed at 1 TPa.

micrometers, suggesting that $10^{-4} < s < 10^{-2}$ might be possible[59] (blue region, Figure 5b) and that greater stiffening can be achieved. This is further evident from a phase diagram of composite stiffness as a function of: 1) the nanofiller aspect ratio; and 2) the contrast between hydrogel and filler stiffness.

At the low volume fractions associated with nanofillers, E_c varied linearly with [GO] at various modulus ratios and aspect ratios (Figure 5c,d), so that the effect of filler could be understood through an effective modulus E_{eff} in a rule of mixtures[36] relationship:

$$\frac{E_c}{E_m} = 1 + \left(\frac{E_{eff}}{E_m} - 1\right) v_f \tag{3}$$

where $v_f = [GO]/\rho_{GO}$ is the volume fraction of the nanofiller, ρ_{GO} is the density of GO, and E_{eff} accounts for modulus, aspect ratio, and surface energy effects. When $E_{eff} = E_f$, Equation (3) is the Voigt upper bound.

Then, we try to find an explicit expression of the slope (E_{eff}/E_m) in Equation (3). From the Mori–Tanaka homogenization theory (Equation S20, **Supporting information**) and Equation (3), the Young's modulus of a composite can be written:

$$\frac{E_c}{E_m} = \frac{3K_m + G_m}{3K_m\left(1 + v_f q\right) + G_m\left(1 + v_f p\right)} = 1 - \frac{\left(3K_m q + G_m p\right) v_f}{3K_m + G_m + \left(3K_m q + G_m p\right) v_f} \tag{4}$$

For small volume fraction v_f, Equation (4) could be simplified as:

$$\frac{E_c}{E_m} = 1 - \frac{3K_m q_2 + G_m p_2}{3K_m + G_m} v_f \equiv 1 + \left(\frac{E_{eff}}{E_m} - 1\right) v_f \tag{5}$$

so that the effective rule-of-mixtures modulus of the filler nanoparticles (E_{eff}) could be written:

$$\frac{E_{eff}}{E_m} = 1 - \frac{3K_m q_2 + G_m p_2}{3K_m + G_m} \tag{6}$$

Through Equation (6), we calculated contours of E_{eff}/E_m and E_{eff}/E_f as a function of aspect ratio s and modulus ratio E_f/E_m

(Figure S1, Supporting Information). It showed that parameter space could be segmented into two regions divided by the line $E_f/E_m = 1/s$ (dotted lines, (Figure S1, Supporting Information). For $E_f/E_m > 1/s$ (the upper half of the plot), E_{eff}/E_m was "shape-limited" depending more on aspect ratio than on modulus ratio. For $E_f/E_m < 1/s$ (the lower half of the plot), E_{eff}/E_m was a "modulus-limited region" depending more on modulus ratio than on aspect ratio. GO-OEGDA, with E_f/E_m ($>10^6$) greater than $1/s$ ($<10^4$), fell into the shape-limited region. In "modulus-limited region" E_{eff} could exceed $0.25E_f$, which was near the Voigt upper bound for composite. In the shape-limited region, $E_{eff} \ll E_f$, and the mechanical properties of composite cannot fully exert the 1 TPa Young's modulus of GO.

Important hypotheses to test are that the loss of stiffness with increasing nanofiller concentration arose from aggregation of particles that may have effectively introduced voids into or attenuated percolation of the GO-OEGDA hydrogels, or that large or poorly bonded interfacial layers may have been a factor. To test these hypotheses, TEM analysis of GO-OEGDA hydrogels and their internal interfaces were performed (representative data from 8 images in 2 specimens in Figure S2, Supporting Information). TEM analysis did not support these countervailing hypotheses. In all images, GO was dispersed homogenously and uniformly in the OEGDA matrix, similar to previous observations in GO-epoxy nanocomposites.[51] GO bonded strongly with OEGDA matrix across all acrylate conversion levels considered ($60\% < P_{CC} < 100\%$), with no transition zones or agglomerations visible. Because the GO-OEGDA interface was well defined, continuous, and thin for all levels of gelation, and no agglomerations were evident, the anomalous loss of stiffness we observed was unlikely to have arisen from nanofiller aggregation or inefficient GO-OEGDA binding.

To test the importance of surface energy effects for GO-OEGDA, we recalculated GO-OEGDA nanocomposite moduli using a homogenization scheme that accounted for these effects using a Gurtin–Murdoch type model. The nanocomposite bulk modulus K_c was only weakly dependent upon the nanofiller characteristic length scale l_1 for the range of parameters appropriate for GO-OEGDA (≈3% difference in the range of $l_1 \approx 0.3$ nm and [GO] = 11.6 mg ml^{-1}) (Figure S3, Supporting Information). These results suggest that the gelation kinetics-coupled MT estimate is sufficient for predicting GO-OEGDA nanocomposites.

3. Conclusion

In conclusion, optical effects, combined with the multi-faceted surface chemistry of GO and its effects on gelation kinetics, can lead to composite hydrogels whose stiffness does not increase monotonically with the addition of a nanofiller. Our combined model of gelation kinetics, surface energy, and micromechanics describes these relationships, and more broadly predicts how synthesis parameters (i.e., precursor compositions, crosslinking conditions, shape and mechanical properties of nanofillers) combined with synthesis conditions to give rise to the final Young's modulus of a composite hydrogel. Results revealed how gelation kinetics predict composite mechanics, including the anomalous decreases in stiffness with the addition of a stiff filler. Although in our material system the effect of surface energy on mechanics was found to be minimal, it is substantial in other nanocomposites. In such cases, approaches based upon the Gurtin–Murdoch model would be appropriate instead of the Mori–Tanaka estimate. With an appropriate choice of homogenization model, the general framework could be utilized to design a range of nanoparticle-doped hydrogel material systems.

Supporting Information

Supporting Information is available from the Wiley Online Library or from the author.

Acknowledgements

This work was supported by the National Natural Science Foundation of China (11772253, 12022206, 11532009), the Shaanxi Province Youth Talent Support Program, the Young Talent Support Plan of Xi'an Jiaotong University, the National Institutes of Health (R01AR077793).

Conflict of Interest

The authors declare no conflict of interest.

Data Availability Statement

Research data are not shared.

Keywords

gelation kinetics, micromechanics, nanocomposite hydrogels, photo-activated nanocomposites

Received: March 8, 2021
Revised: May 11, 2021
Published online: May 29, 2021

[1] S. Choi, S. I. Han, D. Kim, T. Hyeon, D.-H. Kim, *Chem. Soc. Rev.* **2019**, *48*, 1566.
[2] Y. Ma, M. Lin, G. Huang, Y. Li, S. Wang, G. Bai, T. J. Lu, F. Xu, *Adv. Mater.* **2018**, *30*, 1705911.
[3] C. Yang, Z. Suo, *Nat. Rev. Mater.* **2018**, *3*, 125.
[4] C. Xu, G. Dai, Y. Hong, *Acta Biomater.* **2019**, *95*, 50.
[5] S. Lin, L. Gu, *Materials* **2015**, *8*, 551.
[6] Q. Chen, H. Chen, L. Zhu, J. Zheng, *Macromol. Chem. Phys.* **2016**, *217*, 1022.
[7] P. Lin, S. Ma, X. Wang, F. Zhou, *Adv. Mater.* **2015**, *27*, 2054.
[8] G. Mittal, K. Y. Rhee, V. Mišković-Stanković, D. Hui, *Composites, Part B* **2018**, *138*, 122.
[9] R. Tutar, A. Motealleh, A. Khademhosseini, N. S. Kehr, *Adv. Funct. Mater.* **2019**, *29*, 1904344.
[10] H.-L. Tan, S.-Y. Teow, J. Pushpamalar, *Bioengineering* **2019**, *6*, 17.
[11] C. Zhang, K. Liang, D. Zhou, H. Yang, X. Liu, X. Yin, W. Xu, Y. Zhou, P. Xiao, *ACS Appl. Mater. Interfaces* **2018**, *10*, 27692.
[12] C. Pramanik, D. Nepal, M. Nathanson, J. R. Gissinger, A. Garley, R. J. Berry, A. Davijani, S. Kumar, H. Heinz, *Compos. Sci. Technol.* **2018**, *166*, 86.
[13] K.-Y. Lee, Y. Aitomäki, L. A. Berglund, K. Oksman, A. Bismarck, *Compos. Sci. Technol.* **2014**, *105*, 15.

[14] R. J. Young, I. A. Kinloch, L. Gong, K. S. Novoselov, *Compos. Sci. Technol.* **2012**, *72*, 1459.
[15] L. Z. Zhao, C. H. Zhou, J. Wang, D. S. Tong, W. H. Yu, H. Wang, *Soft Matter* **2015**, *11*, 9229.
[16] H. Yuk, B. Lu, X. Zhao, *Chem. Soc. Rev.* **2019**, *48*, 1642.
[17] S. U. R. Shin, C. Zihlmann, M. Akbari, P. Assawes, L. Cheung, K. Zhang, V. Manoharan, Y. U. S. Zhang, M. Yüksekkaya, K.-T. Wan, M. Nikkhah, M. R. Dokmeci, X. S. Tang, A. Khademhosseini, *Small* **2016**, *12*, 3677.
[18] C. Cha, S. R. Shin, X. Gao, N. Annabi, M. R. Dokmeci, X. S. Tang, A. Khademhosseini, *Small* **2013**, *10*, 514.
[19] H. Zhu, H. Yang, Y. Ma, T. J. Lu, F. Xu, G. M. Genin, M. Lin, *Adv. Funct. Mater.* **2020**, *30*, 2000639.
[20] C. N. Bowman, C. J. Kloxin, *AIChE J.* **2008**, *54*, 2775.
[21] H. Zhu, X. Yang, G. M. Genin, T. J. Lu, F. Xu, M. Lin, *J. Mech. Behav. Biomed. Mater.* **2018**, *88*, 160.
[22] H. Zhu, X. Yang, G. M. Genin, T. J. Lu, F. Xu, M. Lin, *J. Mech. Phys. Solids* **2020**, *142*, 104041.
[23] C. Altinkok, T. Uyar, M. A. Tasdelen, Y. Yagci, *J. Polym. Sci., Part A: Polym. Chem.* **2011**, *49*, 3658.
[24] H. Roghani-Mamaqani, V. Haddadi-Asl, M. Najafi, M. Salami-Kalajahi, *J. Appl. Polym. Sci.* **2012**, *123*, 409.
[25] I. S. Tsagkalias, S. Papadopoulou, G. D. Verros, D. S. Achilias, *Ind. Eng. Chem. Res.* **2018**, *57*, 2449.
[26] I. Tsagkalias, V. Proskynitopoulou, G. Verros, D. S. Achilias, *Mater. Today: Proc.* **2018**, *5*, 27517.
[27] M. Sadej, E. Andrzejewska, *Prog. Org. Coat.* **2016**, *94*, 1.
[28] M. N. Siddiqui, H. H. Redhwi, G. D. Verros, D. S. Achilias, *Ind. Eng. Chem. Res.* **2014**, *53*, 11303.
[29] I. Tsagkalias, A. Vlachou, G. Verros, D. Achilias, *Polymers* **2019**, *11*, 999.
[30] G. W. Milton, *The Theory of Composites*, Cambridge UP, Cambridge **2002**, p. 748.
[31] Q. H. Zeng, A. B. Yu, G. Q. Lu, *Prog. Polym. Sci.* **2008**, *33*, 191.
[32] S. Torquato, *Random Heterogeneous Materials: Microstructure and Macroscopic Properties*, Springer Science & Business Media, New York **2005**.
[33] Y. Ni, M. Y. M. Chiang, M. Y. M. Chiang, *J. Mech. Phys. Solids* **2007**, *55*, 517.
[34] F. Saadat, V. Birman, S. Thomopoulos, G. M. Genin, *J. Mech. Phys. Solids* **2015**, *82*, 367.
[35] A. Reuss, *Z. Angew. Math. Mech.* **1929**, *9*, 49.
[36] W. Voigt, *Ann. Phys.* **1889**, *274*, 573.
[37] Z. Hashin, S. Shtrikman, *J. Mech. Phys. Solids* **1963**, *11*, 127.
[38] Z. Hashin, S. Shtrikman, *J. Mech. Phys. Solids* **1962**, *10*, 335.
[39] G. W. Milton, N. Phan-Thien, *Proc. R. Soc. London, Ser. A* **1982**, *380*, 305.
[40] R. Hill, *J. Mech. Phys. Solids* **1965**, *13*, 213.
[41] B. Budiansky, *J. Mech. Phys. Solids* **1965**, *13*, 223.
[42] J. C. H. Affdl, J. L. Kardos, *Polym. Eng. Sci.* **1976**, *16*, 344.
[43] J. E. Shin, H. W. Kim, B. M. Yoo, H. B. Park, *J. Appl. Polym. Sci.* **2018**, *135*, 45417.
[44] T. Mori, K. Tanaka, *Acta Metall.* **1973**, *21*, 571.
[45] G. P. Tandon, G. J. Weng, *Compos. Sci. Technol.* **1986**, *27*, 111.
[46] G. P. Tandon, G. J. Weng, *Polym. Compos.* **1984**, *5*, 327.
[47] G. J. Weng, *Int. J. Eng. Sci.* **1990**, *28*, 1111.
[48] A. Hussein, B. Kim, *Compos. Struct.* **2018**, *202*, 170.
[49] J. D. Eshelby, *Proc. R. Soc. London, Ser. A* **1957**, *241*, 376.
[50] Z. Liu, J. A. Moore, W. K. Liu, *J. Mech. Phys. Solids* **2016**, *95*, 663.
[51] W.-S. Kang, K. Y. Rhee, S.-J. Park, *Composites, Part B* **2017**, *114*, 175.
[52] C. Sun, Y. Huang, Q. Shen, W. Wang, W. Pan, P. A. Zong, L. Yang, Y. Xing, C. Wan, *Sci. Adv.* **2020**, *6*, eabb1338.
[53] V. A. Eremeyev, *Acta Mech.* **2015**, *227*, 29.
[54] R. Dingreville, A. Hallil, S. Berbenni, *J. Mech. Phys. Solids* **2014**, *72*, 40.
[55] Y. Yao, S. Chen, D. Fang, *J. Mech. Phys. Solids* **2017**, *99*, 321.
[56] Y. Yao, Z. Peng, J. Li, S. Chen, *J. Appl. Mech.* **2019**, *87*, 021008.
[57] R. J. Young, M. Liu, I. A. Kinloch, S. Li, X. Zhao, C. Vallés, D. G. Papageorgiou, *Compos. Sci. Technol.* **2018**, *154*, 110.
[58] D. G. Papageorgiou, I. A. Kinloch, R. J. Young, *Prog. Mater. Sci.* **2017**, *90*, 75.
[59] Z.-K. Cui, S. Kim, J. J. Baljon, B. M. Wu, T. Aghaloo, M. Lee, *Nat. Commun.* **2019**, *10*, 3523.